

An Active Ripple Filtering Technique for Improving Common-Mode Inductor Performance

Pádraig Cantillon-Murphy, *Student Member, IEEE*, Timothy C. Neugebauer, *Student Member, IEEE*, Claudio Brasca, *Student Member, IEEE*, and David J. Perreault, *Member, IEEE*

Abstract—Active ripple filtering is the replacement of large passive components in power filter circuits with smaller passive components and active control circuitry. This letter focuses on common-mode filters, where a large common-mode inductor (choke) is replaced by two smaller chokes and active op-amp control. The technique is appropriate when improved attenuation is required at relatively low frequencies and the high-frequency filtering requirements are easily met. Smaller chokes save significantly in material and winding costs. The technique is more advantageous if wire-wound chokes can be replaced by planar printed circuit board chokes. The use of the technique in an automotive electromagnetic interference (EMI) filter application is explored in detail.

Index Terms—Active filtering, choke, common-mode inductor, electromagnetic interference filter.

I. INTRODUCTION

THE SIZE and cost of electromagnetic interference (EMI) filter components are important considerations in many power applications. One approach to reducing passive filter component size is the use of an active ripple filter. An active ripple filter replaces large passive components with smaller passives and some active control circuitry. Techniques exist to either reduce the amount of noise that is generated, or to improve the performance of the passive filter [3]–[17]. This letter introduces a filtering method which replaces a large choke with two smaller chokes and some active op-amp control circuitry. This substitution can lead to an improvement in the filter's attenuation performance over a specified frequency range. An application in the AM frequency band is examined, where the frequency range of interest is from 150 kHz to 1.7 MHz. At frequencies greater than the bandwidth of the op-amp, the filter again performs as a passive component.

The technique is appropriate when the size of the filter's choke is determined by the attenuation requirements at the low end of the specified frequency range. The two smaller chokes which replace it result in significant material and winding savings. The letter also highlights the benefits of replacing wire-wound chokes with planar printed circuit board chokes. This approach is possible because the number of turns required to achieve a certain attenuation is reduced using the active technique. A planar choke also reduces the problem of distributed capacitance, which arises in the wire-wound design.

Manuscript received January 14, 2004; revised May 17, 2004. Recommended by Associate Editor V. G. Agelidis.

The authors are with the Massachusetts Institute of Technology, Cambridge, MA 01239 USA (e-mail: padraig@mit.edu).

Digital Object Identifier 10.1109/LPEL.2004.831155

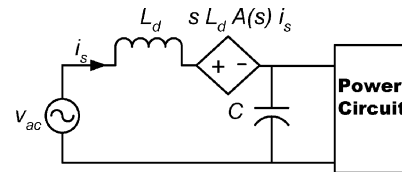


Fig. 1. Inductor enhancement for differential-mode signals.

II. GENERAL TECHNIQUE

The size of a choke in a common-mode filter is determined by the common-mode attenuation requirements of the design. Attenuation increases with common-mode impedance. The corresponding inductance, L , increases with the square of the number of turns on the choke's core, N , according to (1), where A_L is a parameter determined by the core size and material

$$L(\text{in nH}) = A_L N^2. \quad (1)$$

Therefore, for a given core size and material, the impedance to common-mode signals is usually increased by adding more turns. This is limited by the window area of the selected core. An increase in the common-mode attenuation requires larger chokes with more window area to fit the extra turns. The active common-mode filter presented here increases the filter's common-mode attenuation without adding extra turns. This results in significant size and cost reductions.

Many types of active ripple filters are possible. Ripple-current filters reduce the ripple current passing through a circuit branch [7]–[15] while ripple-voltage filters reduce the ripple voltage at a circuit node [9], [10], [16], [17]. Feedforward filters achieve ripple reduction by measuring a ripple component and injecting its inverse [7], [12]–[14], [16], while feedback filters operate to suppress the ripple with high-gain feedback control [8]–[11], [13], [15]–[17]. Hybrids of these filter types are also possible (see [8], [13], [16]). Even within a given active filter type there are many possible ways to implement the required sensing and driving functions.

The application in this letter uses a ripple voltage filter, since sensing voltage signals is less costly than current signals and cost is a critical factor in the example application. The technique, as applied to differential signals, is shown in Fig. 1. An active voltage source is placed in series with the inductor whose value is to be increased. This causes the inductance value to appear $1 + A(s)$ times its original value. Here, $A(s)$ is the frequency-dependent amplifier gain. The method keeps the inductor from seeing the full magnitude of the capacitor's ripple voltage and the corresponding ripple current at the output is reduced. In addition, this active technique increases the point

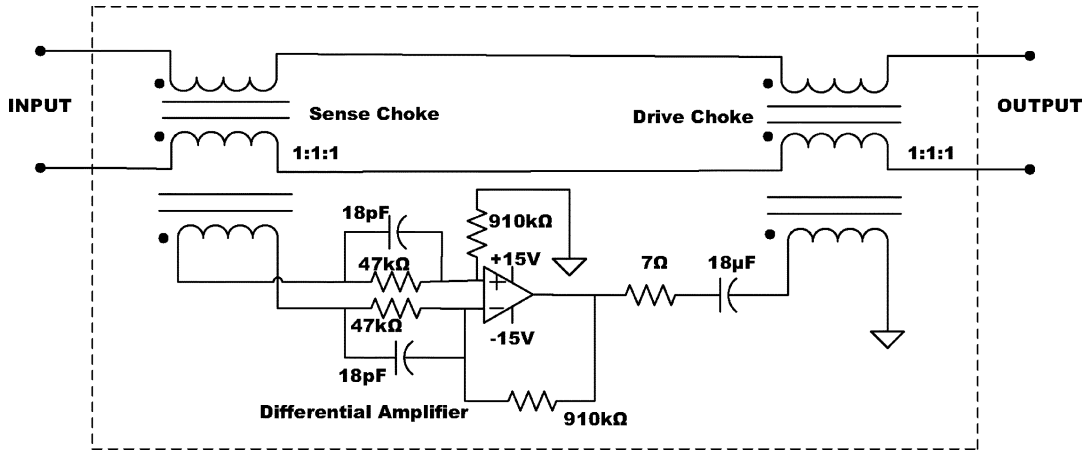


Fig. 2. Proposed active common-mode choke.

impedance, which is important in the application considered here. Ripple voltage sensing is achieved using a high input-impedance amplifier which amplifies the ripple voltage across the sense inductor. This letter explores the application of the differential mode technique in Fig. 1 to common-mode signals, where the differential mode inductor is replaced by a common-mode choke.

III. IMPLEMENTATION CONSIDERATIONS

Fig. 2 shows the full circuit structure and implementation of the active common-mode choke while the circuit of Fig. 3 represents a simplified model of the proposed common-mode choke. This active choke comprises a sense choke, a drive choke and an amplifier which applies an amplified version of the sensed common-mode voltage, v_1 , across the drive choke. The sense and drive inductances, $L_{\mu 1}$ and $L_{\mu 2}$ respectively, are the intrinsic magnetizing inductances of the sense and drive chokes. The voltage across the sense inductance is measured via a sense winding and amplified by the frequency-dependent gain $A(s)$, using an op-amp, although discrete active devices could also be used. Simple voltage and current analysis leads to the general expression for the input impedance of the system given in (2), in terms of $L_{\mu 1}$ and $A(s)$

$$Z_s = \frac{v_s}{i_s} = sL_{\mu 1}\{A(s) + 1\}. \quad (2)$$

The two design parameters are $L_{\mu 1}$ and $A(s)$. Typically $A(s)$ is a large constant at low frequency and approaches zero at high frequency. Therefore, the system could be designed to make the input impedance in Fig. 3 appear 10 to 20 times larger up to frequencies around 1 MHz using inexpensive gain-bandwidth op-amps. This increase in input impedance is not found in some related active filter designs (e.g., [17]), and is important for the application considered here.

One would expect the additional parameter of the sense choke's turns ratio to facilitate an extra degree of freedom in selecting $A(s)$. In practice, this is limited by cross-winding capacitive effects on the sense choke. Two steps are suggested to minimize the impact of this capacitance: 1) configuring the op-amp as a differential amplifier and 2) minimizing the turns ratio of the sense choke so that $A(s)$ is only contributed by the

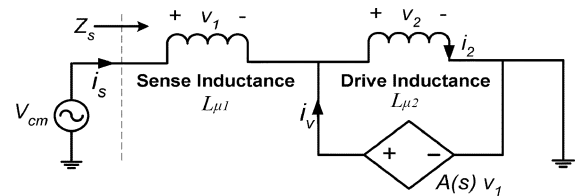


Fig. 3. One half of the proposed common-mode choke.

op-amp. These techniques are explored in detail in the context of the example application.

Neglecting v_1 , which is relatively small compared to the drop v_2 across the drive inductance, the current flowing through the active source in Fig. 3 is given by (3)

$$i_v \approx \frac{A(s)v_1}{sL_{\mu 2}}. \quad (3)$$

Clearly, the limiting factor on the size of this drive inductance is not the magnetizing inductance, as in the case of the sense choke, but the amount of current sourced by the amplifier. Also, the main windings on the drive choke should be thick enough to accommodate dc currents at the system input. These factors determine the required window area for the drive choke, and allow the minimum value of $L_{\mu 2}$ to be much smaller than $L_{\mu 1}$. Therefore, a much smaller choke than the sense choke could be used to implement the drive inductance, with associated cost and weight benefits.

To summarize, a large choke is replaced with two smaller chokes, a sense choke and a drive choke, along with active op-amp control. The size of the sense choke is a critical system parameter while the drive choke can be substantially smaller. If we assume that winding cost is a significant portion of the original choke's cost, some savings result from using this technique.

The benefits of this technique are more dramatic when we replace the wire-wound chokes with planar chokes, where the windings are traces on a printed circuit board. The attenuation required in common-mode applications generally does not allow for this, because the size of the magnetizing inductance required for reasonable common-mode attenuation means that a large number of turns are needed. Printed circuit design of

common-mode filters is only possible if the number of choke turns has been reduced to the point where implementation on a printed circuit board is feasible. This is accomplished using the active filtering technique. For chokes with printed windings, the winding costs are eliminated. Also, the cross-winding capacitance can be easily controlled allowing a larger turns ratio on the sense choke, should it be required.

IV. EXAMPLE APPLICATION

This application examines a choke used for filtering frequencies in the AM range between 150 kHz and 1.7 MHz. The choke is part of a design which uses the rear-window electrical heater element of a motor-vehicle as the vehicle's radio antenna. The circuit proposed in [2] is shown in Fig. 4. A switched dc electrical network is provided for connection to the battery, such that the power dissipated in the element's resistance heats the window. At the same time, at high ac frequency, the element is used as a radio antenna. Common-mode filtering is needed to prevent RF disturbances on the electrical network from interfering with radio reception, to prevent loading of the antenna at RF frequencies and to prevent RF signals picked up by the antenna from being injected into the electrical network. The common-mode choke, labeled $L3$ in Fig. 3, is a particularly large and expensive item in this system. It must both carry the large dc heater current and have high impedance over the AM frequency range [2]. The far smaller inductors, $L1$ and $L2$, are for filtering in the FM band, and can be neglected for our present purposes.

The choke should be capable of carrying a dc current of 20 A with a ripple voltage whose amplitude does not exceed 50 mV. It should present a common-mode impedance of greater than 1 k Ω to the windshield antenna over the entire AM range. This requires a minimum common-mode inductance of 1 mH, in order to meet the specifications at 150 kHz. One passive choke solution is a packed RM 12 core of N30 material which is large, heavy, and represents a large fraction of the overall circuit cost.

This letter proposes the active choke of Fig. 2 to replace this large passive 1 mH choke. The packed RM 12 choke is replaced by two unity-gain RM 8 cores of 3F3 material and active op-amp control. The application uses identical sense and drive chokes for convenience. However, as noted already, this need not be the case since it should be expected that the size of the drive choke can be significantly smaller without affecting filter performance. The two RM 8 cores are each designed with magnetizing inductances of 50 μ H and the dc system gain, $A(s)$, is set at 20.

Because of the cross-winding capacitance that appears in each choke, $A(s)$ is only contributed by the amplifier. This cross-winding capacitance arises between the power windings, which carry both ac and dc input signals, and the control windings, which carry just the reflected ac signals. In Fig. 2, the power windings are those with a physical connection to the system input and output terminals, while the control windings are those connected to the amplifier input and output. Since the sense choke is coupled to the amplifier input, the capacitive effect is particularly critical there. If the number of turns of control windings on the sense choke is increased, the problem is amplified since there is more available area for capacitance effects. Therefore, to minimize its impact, the turns ratio of the

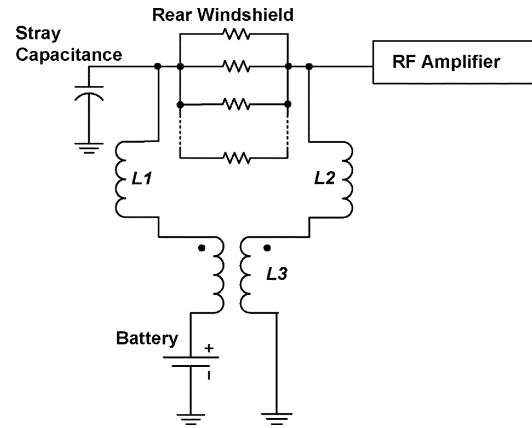


Fig. 4. Proposed passive solution for a combined electrical window heater and radio antenna.

sense choke is chosen to be unity. The turns ratio of the drive choke is also selected as unity.

With the core size and material chosen, it can be shown from (1) that four turns are required for an inductance of around 50 μ H, since the A_L value for 3F3 material and an RM 8 core is 3000. In reality this inductance was measured as 36 μ H for the drive choke and 38 μ H for the sense choke. The common-mode power signals on each choke are carried on two 14 AWG windings, each with four turns. For the control signals, 32 AWG windings are sufficient, since there is no high dc current.

The op-amp is configured as a standard differential amplifier. This configuration also helps to minimize the effects of cross-winding capacitance between the power and control windings on the sense choke. First, consider the case of a standard inverting or noninverting op-amp configuration. If the op-amp amplifies the reflected ripple-voltage with respect to ground, there exists a relatively low impedance path to ground seen from one of the amplifier inputs. The power windings also see a path to the same signal ground. This current path contributes to the cross-winding capacitance between the control and power windings and results in distortion of the amplifier's frequency response. Using a differential amplifier means both amplifier inputs see a virtual open circuit and the current path that arises in the simple amplifier case is minimized. For this reason, a differential amplifier is used to amplify the reflected common-mode ripple-voltage and a unity turns-ratio is employed to maintain a low cross-winding capacitance on both wire-wound chokes.

The amplifier has a dc gain of 20. There are many possible op-amps suitable for this application but in an automotive environment, cost is critical. Therefore, the low-cost LF 356 op-amp, with a gain-bandwidth of 5 MHz is selected as the most suitable. This device has an intrinsic two-pole rolloff, which should theoretically begin around 250 kHz when the op-amp is arranged with a dc gain of 20. In practice, the rolloff is found to begin closer to 150 kHz and some temperature dependence of this corner frequency is possible. This intrinsic two-pole rolloff is used in the design of Fig. 2. The two 18 pF capacitors, connected in parallel across the amplifier's input resistors, introduce a zero at 150 kHz and a high-frequency pole. The result is a pole rolloff characteristic at low frequency while system stability is maintained.

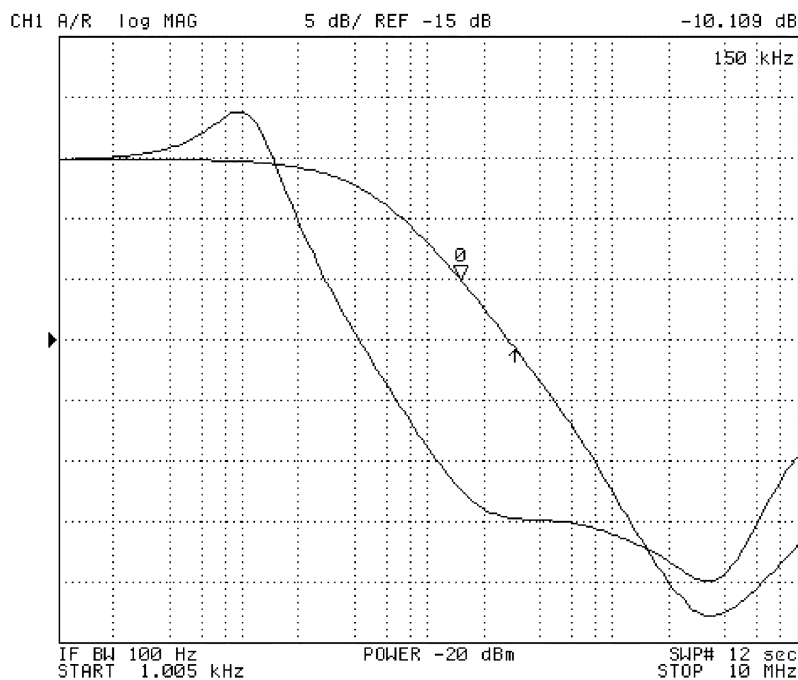


Fig. 5. System attenuation with and without active filtering for the wire-wound design.

In an application where cost is not so crucial, a wide-bandwidth op-amp could be used to significantly improve the performance. This could also eliminate the temperature dependence intrinsic to the design, due to the possibility of the zero at 150 kHz not being perfectly matched to the op-amp's dynamics across temperature. A wide-bandwidth op-amp with a compensating pole, instead of a zero at 150 kHz, would alleviate this possible dependence.

An R-C series network is inserted at the output of the op-amp to minimize the dc offset associated with the LF 356. Its time constant is chosen to be well below the AM range. The amplifier is powered at ± 15 V, making implementation in an automotive environment feasible. An offset biasing scheme could be readily used to eliminate the necessity for a separate negative supply, thus enabling the system to be powered from the vehicle's battery.

The performance of the circuit in Fig. 2, under light load and without any dc (differential-mode) current present, is shown in Fig. 5. The system's frequency response is analyzed by injecting a common-mode ripple voltage at the input and comparing this signal with the output across a 50Ω resistive load. Each common-mode branch has a separate 50Ω load termination. With the op-amp powered off, each branch of the power windings corresponds to an equivalent input impedance of 136Ω at 150 kHz (by the series combination of the two magnetizing inductances). Powering on the op-amp increases this series combination due to a gain of $1 + A(s)$ in the size of the drive choke's magnetizing inductance. The voltage across one of the 50Ω load resistors normalized with respect to the input voltage is plotted between 1 kHz and 10 MHz, with and without the active filtering powered on. The results are shown in Fig. 5.

At low frequency, both configurations result in similar performance. However, by 150 kHz, the active filter circuit im-

proves attenuation by 17 dB over the passive-only case. At high frequency, the active filtering is no longer effective and performance reverts to what would be achieved by the passive components acting alone. The dot convention of Fig. 4 is worth noting. For an incremental voltage in the positive direction across the drive choke, the coils need to be wound as the convention indicates. Otherwise, active voltage addition is not achieved.

Clearly, this technique of active filtering can substantially reduce the number of turns required to fulfill the attenuation specifications for a common-mode filter, particularly if the filter specifications are defined by low-frequency performance. This allows the designer to investigate choke implementation using two planar chokes, where the windings are traces on a printed circuit board.

The circuit used to demonstrate this is a two-sided board with 1oz. copper, though multi-layer designs with heavier copper would likely be preferable in practice. Again, the magnetizing inductances of the sense and drive chokes from Fig. 4 are equal but, this time, designed and measured to be $35 \mu\text{H}$. The core material is 3F3 and the RM 8 cores are replaced by planar E cores.

Various combinations of planar E core sizes and the number of turns required for an inductance of $35 \mu\text{H}$ can be used. This combination is based on the A_L values for different 3F3 core sizes [17]. The possibilities are increased further if a multilayer board is available. In this two-layer design, the E64 core is selected so that two turns suffice for a magnetizing inductance of $35 \mu\text{H}$. The design requires 300 mil copper traces to accommodate the 20 A dc differential mode current within a maximum temperature rise of 45°C . A 1:1:1 turns ratio is assumed with 20 mil wide control windings and 20 mil spacing.

The frequency response of this new planar configuration is investigated in an identical manner to the wire-wound case. The results of Fig. 6 show the attenuation with and without the op-amp powered on. The attenuation of the active planar



Fig. 6. System attenuation with and without active filtering for the planar design.

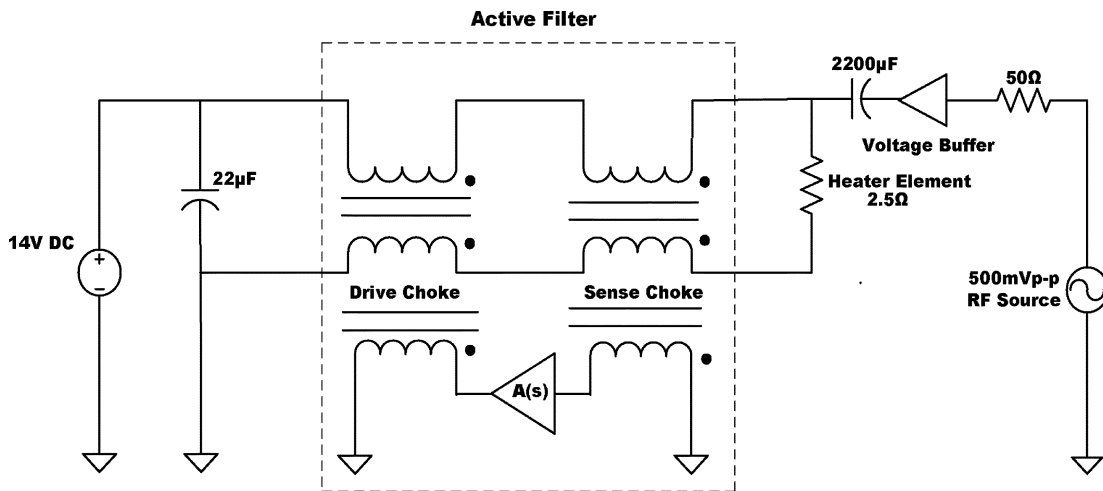


Fig. 7. Circuit used for analysis under dc load conditions.

design at 150 kHz is 20 dB greater than the attenuation with the series combination of the two $35 \mu\text{H}$ chokes. This exceeds the performance of the wire-wound chokes by 3 dB for roughly similar values of magnetizing inductances.

The active planar design is also investigated under dc load conditions, with the arrangement of Fig. 7. This is an attempt to recreate the circuit of Fig. 2 in a test environment, where the rear-window heating element is modeled by a 2.5Ω resistor. A 14 V source is applied to the circuit resulting in a dc current of 5.3 A flowing through the power windings of the sense and drive chokes. The dc signal path is formed by the upper and lower branches of the two chokes' power windings and the 2.5Ω load resistor. A ripple voltage, representing the RF signal, is injected at the load.

The time-domain transient signals resulting from dc load tests performed at 150 kHz are shown in Fig. 8. This frequency

is chosen since it is the lowest frequency of interest in the AM band. Although the actual RF voltage amplitude is not expected to exceed 50 mV, a signal amplitude of 500 mV is used to allow easier inspection of the filter's attenuation with and without active filtering. The left trace describes the voltage and current at the buffer output when the control circuitry is powered off, so that the attenuation in each branch is only due to the two series-connected $35 \mu\text{H}$ inductances. The right trace shows the same signals with the active filter powered on. The voltage buffer ensures that the ripple voltage is consistent in both cases. However, the ripple-current's amplitude falls from 9.04 mA when the active filter is powered off, to 0.88 mA, when it is powered on. This demonstrates an increase in the input impedance of 20 dB at 150 kHz which corresponds with the improvement in attenuation noted at 150 kHz in the frequency response curve of Fig. 6.

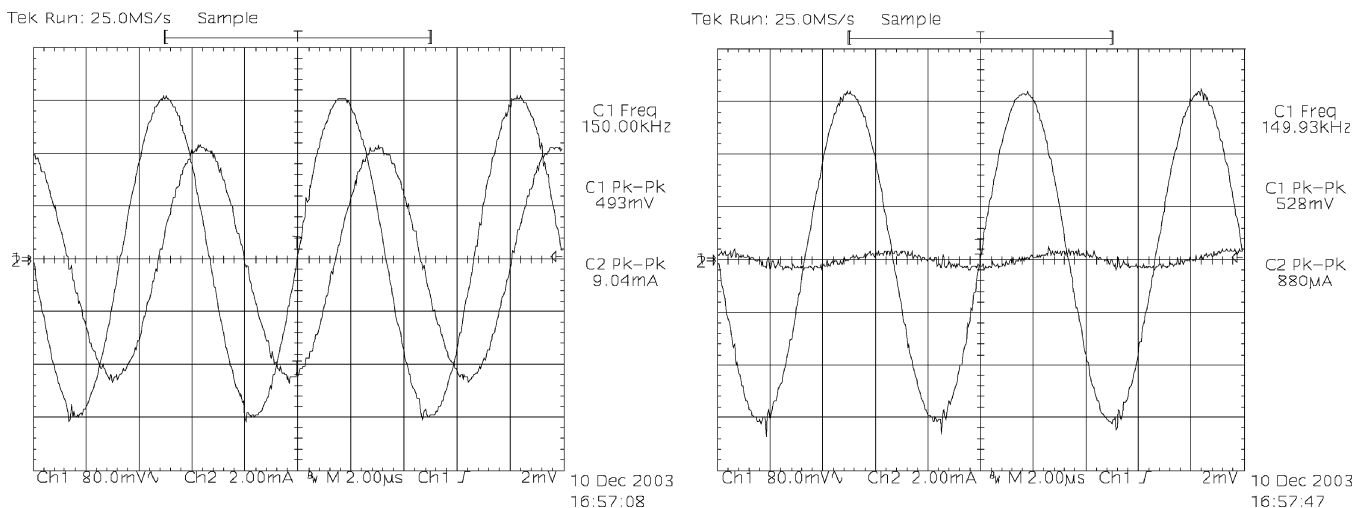


Fig. 8. Time-domain analysis results showing system voltage and current (right) with and (left) without active filtering.

V. CONCLUSIONS

An innovative common-mode inductor enhancement approach is presented that provides increased common-mode impedance and filtering. This approach appears to be particularly advantageous in the case where wire-wound chokes can be replaced by planar chokes. The letter explores an application in the automotive environment where the parasitic magnetizing inductances of two chokes were used to replace a single, larger choke. This letter highlights a 17 dB improvement in attenuation over completely passive circuitry using two small wire-wound chokes at 150 kHz. This increases to 20 dB if the design is implemented with planar chokes. Use of the proposed approach in an automotive EMI filter application is considered in detail.

The dependence of the design on the size of the drive choke was not explored in detail. It is anticipated that the size of the drive choke could be substantially reduced. Furthermore, in printed planar choke implementation, it is anticipated that higher sense-choke turns ratios are likely possible, allowing further attenuation improvement and component size reduction. The proposed technique therefore offers even greater size and cost reductions than have been demonstrated thus far.

REFERENCES

- [1] C. Brasca, "Active RF choke research," in *Confidential Communication*. Montecavolo, Italy: Zendar, 2001.
- [2] B. E. Kropielnicki and J. J. Kropielnicki, "Electrical Device to Enable the Heating Element of an Electrically Heated Motor Vehicle Window to be Used as a Radio Aerial," British Patent 1 520 030, Aug. 2, 1978.
- [3] T. K. Phelps and W. S. Tate, "Optimizing passive input filter design," in *Proc. Powercon 6*, May 1979, pp. G1-1-G1-10.
- [4] M. J. Nave, *Power Line Filter Design for Switched-Mode Power Supplies*. New York: Van Nostrand Reinhold, 1991.
- [5] "Common Mode Filter Design Guide," Coilcraft, Inc., Cary, IL, Rep. Document 191-1, 1997.
- [6] "Common Mode Filter Inductor Analysis," Coilcraft, Inc., Cary, IL, Rep. Document 200-1, 1998.
- [7] M. Zhu, D. J. Perreault, V. Caliskan, T. C. Neugebauer, S. Guttowski, and J. G. Kassakian, "Design and evaluation of an active ripple filter with Rogowski-coil current sensing," in *Proc. IEEE Power Electronics Specialists Conf.*, 1999, pp. 874-880.
- [8] S. Feng, W. A. Sander, and T. Wilson, "Small-capacitance nondissipative ripple filters for DC supplies," *IEEE Trans. Magn.*, vol. 6, pp. 137-142, Mar. 1970.
- [9] J. Walker, "Design of practical and effective active EMI filters," in *Proc. Poweron 11*, vol. I-3, 1984, pp. 1-8.
- [10] L. E. LaWhite and M. F. Schlecht, "Active filters for 1-MHz power circuits with strict input/output ripple requirements," *IEEE Trans. Power Electron.*, vol. PE-2, pp. 282-290, Oct. 1987.
- [11] T. Farkas and M. F. Schlecht, "Viability of active EMI filters for utility applications," *IEEE Trans. Power Electron.*, vol. 9, pp. 328-337, May 1994.
- [12] P. Midya and P. T. Krein, "Feed-forward active filter for output ripple cancellation," *Int. J. Elec.*, vol. 77, no. 5, pp. 805-818, 1994.
- [13] D. C. Hamill, "An efficient active ripple filter for use in DC-DC conversion," *IEEE Trans. Aerosp. Electron. Syst.*, vol. 32, pp. 1077-1084, July 1996.
- [14] M. S. Moon and B. H. Cho, "Novel active ripple filter for the solar array shunt switching unit," *J. Propulsion Power*, vol. 12, no. 1, pp. 78-82, Jan./Feb. 1996.
- [15] M. T. Thompson and M. F. Schlecht, "High power laser diode driver based on power converter technology," *IEEE Trans. Power Electron.*, vol. 12, pp. 46-52, Jan. 1997.
- [16] A. C. Chow and D. J. Perreault, "Design and evaluation of a hybrid passive/active ripple filter with voltage injection," *IEEE Trans. Aerosp. Electron. Syst.*, vol. 39, pp. 471-480, Apr. 2003.
- [17] Y.-C. Son and S.-K. Sul, "A new active common-mode EMI filter for PWM inverter," *IEEE Trans. Power Electron.*, vol. 18, pp. 1309-1314, Nov. 2003.
- [18] *Soft Ferrites and Accessories—2002 Data Handbook*, Ferroxcube Int. Holding B.V, Hamburg, Germany, 2002.